Science of Sintering, **45** (2013) 107-116

doi: 10.2298/SOS1301107C

UDK 543.645

Pore Geometry of Ceramic Device: the Key Factor of Drug Release Kinetics

B. Čolović, D. Milivojević, B. Babić-Stojić, V. Jokanović[*)]
Institute of Nuclear Sciences "Vinča", Laboratory for radiation chemistry and physics, Mike Petrovića Alasa 12-14, University of Belgrade, 11001 Belgrade, Serbia

Abstract:

Release kinetics of tigecycline, a potential antibiotic in treatment of osteomyelitis, from calcium hydroxyapatite (CHA), as one of the most important ceramic materials in bone tissue engineering, was investigated in this study. Tigecycline, in solid state, was mixed with CHA powder and the obtained mixture was compressed into tablets using two different pressures. These tablets were immersed in a phosphate-buffered saline solution and tigecycline release was measured by a UV-VIS spectrophotometer. The total release time was 5 or 28 days, depending on the pressure applied during compression. It was shown that there is a close relationship between pore sizes and drug release rate. The drug release kinetics was interpreted on the base of pore sizes and pore size distribution.

Keywords: *Hydroxyapatite, Pore geometry, Drug release*

1. Introduction

CHA scaffolds have been widely used as implants in dentistry and orthopedics due to their biocompatibility with bone tissue and osteoconductivity [1-3]. Besides, CHA can be used as carrier for drug delivery since it is able to absorb different chemical species on its surface [4, 5]. Bacterial infections occur frequently during surgical interventions and antibiotic administration at the surgical site is of great importance in bone graft surgery because the conventional route of antibiotic administration results in low antibiotic level in the bone tissue, due to limited antibiotic penetration to the bone [6-8]. High local concentrations of antibiotic can be achieved by entrapping the antibiotic into an apatite scaffold, from which it would gradually release and ensure protection from bacterial infections over a long postoperative period [7, 9, 10]. Thus, CHA acts at the same time as a bone substitute material and as a drug delivery device.

Many bone infections are caused by multi-resistant microorganisms and new antimicrobials are needed to repress these resistant bacteria. Therefore, a new class of antibiotics, glycylcycline antibiotics, has been developed to overcome the resistance to tetracyclines. Best known among them is tigecycline, which seems to be a potential drug in treatment of severe orthopedic infections [11-14]. The efficacy of tigecycline in a variety of animal infection models for osteomyelitis, endocarditis, pneumonia and peritonitis was shown in several studies. When applied in humans, tigecycline was widely distributed in the body but its concentration in bone was relatively low, as some studies have shown [12, 14]. One

[*)] **Corresponding author**: vukoman@vinca.rs

study on humans has shown that tigecycline may be used in treatment of chronic osteomyelitis resistant Acinetobacter sp [11].

Drug release kinetics from CHA cements has not been completely clarified yet and none of the existing models describes the whole kinetics of release [1, 15-17]. According to many authors, the kinetics of drug release at the initial stage is controlled by surface phenomenon, while that of sustained release depends on the penetration depth determined by the cement porosity. Thus, the kinetics of drug release is related to the pore size and pore size distribution in the cement used [18-21].

2. Materials and methods

2.1. Materials

The apatite powder used in this study was synthesized as follows. First, two precursor solutions were prepared: (i) 500 ml of 3.02 cmol aqueous suspension of $Ca(OH)_2$ and (ii) 500 ml of 2.32 cmol aqueous solution of $(NH_4)_2HPO_4$. Then, the $(NH_4)_2HPO_4$ solution was poured into the $Ca(OH)_2$ suspension and vigorously stirred. The pH of the so-prepared solution mixture was adjusted to 7.4. Finally, this mixture was transferred into a beaker, covered with a glass plate, and autoclaved at a temperature of 150 ^oC and pressure of 5 bar for 8 h. After hydrothermal treatment in the autoclave, the precipitate was decanted, dried at 80 ^oC for 48 h, ground, washed with deionized water, and ultracentrifuged in order to obtain the purest possible CHA. [22]

2.2. Tablet fabrication

Tigecycline, in concentration of 0.5 % w/w, was mixed with CHA powder and compressed into tablets with a pressure of 16 and 156 MPa, using a hydraulic press. Tablet parameters were: diameter - 10 mm, height -2 mm.

2.3. Tablet evaluation

An X-ray diffraction (XRD) method (Philips PW 1050) with Cu-Kα1−2 radiation was used for phase analysis of CHA and determination of crystallite sizes and lattice parameters. Data were analyzed in the range of 2θ from 9 to 67◦ with a scanning step of 5◦, and exposition time of 2 sec per a step [22].

A PERKIN ELMER 983G IR spectrometer, with KBr pastille, was used for CHA powder characterization. IR spectra were recorded in the wave number range of 4000–400 cm^{-1}.

A scanning electron microscope (SEM JEOL 5300) was used to analyze the morphology and size distribution of CHA particles. Samples for SEM analysis were prepared as follows: they were suspended in ethanol and dispersed by ultrasound for 10 min, and then coated with gold by the PVD process.

Specific surface areas were measured by nitrogen adsorption at −196 °C using a Varian Aerograph (model 920) gas chromatograph equipped with TCD detector. Before the measurements, the samples were treated at 150 °C in a helium flow for 2h. After that, a gas mixture of 27 vol.% of nitrogen in helium (30 cm^3/min) was passed over the sample and the sample cell was cooled by immersion in liquid nitrogen. The cooling sample adsorbed a certain amount of nitrogen from the gas stream until adsorption equilibrium was established. After removal of the liquid nitrogen bath, the sample was warmed and the adsorbed nitrogen released, enriching the effluent monitored by a TCD detector. When desorption was complete,

a known volume of nitrogen (0.5 cm^3) was added to the nitrogen–helium stream. By comparing desorption and calibration peaks, the volume of nitrogen adsorbed by the sample was calculated and the surface area of the sample determined by "one point" BET method. The assumption that the synthesized particles were spheroids enabled the calculation of the average radius of particles (dBET = 6/ρSw), where Sw is the specific surface area and ρ = 3.156 g/cm^3 is the theoretical density of synthesized CHA powders.

Porosimetry measurements were carried out on a Carlo Erba Porosimeter 2000 using the Milestone 200 Software System. This high-pressure mercury intrusion porosimeter operates in the interval 0.1−200 MPa, enabling estimation of pores in the range from 7.5 to 15000 nm.

2.4. Drug release

Tigecycline release was measured after immersion of tablets into 40 ml phosphate buffer saline (PBS) at 37°C and continuous stirring. The quantity of released antibiotic was measured using a UV-VIS spectrophotometer at the wavelength of 245 nm, by taking 3 ml samples at desired time intervals. Withdrawn samples were replaced with 3 ml of fresh PBS.

2.5. Drug release kinetics - general approach

Drug release kinetics depends on many factors: the microstructure of the drug delivery device, drug solubility, type of bond between the drug and the device, and, if any, on the mechanism of device degradation. Calcium phosphate cements can be treated as non-biodegradable devices because the rate of drug liberation is much higher than the rate of matrix degradation. So, the drug release is controlled by the diffusion process through the cement device. [1]

Equations for drug release from diffusion controlled devices are based on Fick's second diffusion law. A well-known is Higuchi's equation, based on a pseudo steady-state approach:

$$M_t = A\sqrt{C_s(2C_0 - C_s)Dt}\ ,$$

where M_t is the amount of drug released for time t; A is the surface area of the device; D is the diffusion coefficient of the drug in the matrix; C_s is the solubility of the drug in the matrix; C_0 is the initial concentration of the drug in the matrix. This equation can describe, at least, the initial phase of the release, when about 60% of the total drug amount is released [1, 15].

The Korsmeyer-Peppas model is also used to describe the drug release kinetics, and it is also applicable to degrading matrices in which the drug release mechanism often deviates from Fick's law, described by the following equation [16]:

$$M_t/M_\infty = kt^n,$$

where M_t is the quantity of drug released at time t, M_∞ is the quantity of drug released at infinite time, k is the kinetic constant, while n is the release exponent (for cylindrical matrices n: 0.43 to 0.5 (diffusion controlled release) and $0.50 < n < 1.0$ (anomalous transport). This model, too, is generally not applicable after 60% of total drug amount is released [16].

3. Results and discussion

3.1. Phase analysis

The obtained X-ray data (Fig.1.) show that the hydrothermally synthesized powder corresponds to carbonated calcium hydroxyapatite $Ca_{10}(PO_4)_6(OH)_2$ (JCPDS 9–432). All

characteristic diffraction patterns are present: (211) at 2θ =31.9°; (112) at 2 θ = 32.26 °, (3 0 0) at 2 θ =33.12 °, (002) at 2 θ = 25.86 °, (222) at 2 θ = 46.86 °, and (213) at 2 θ = 49.58 ° [21]. The crystallites size, calculated using Sherer's equation, is 8-22 nm.

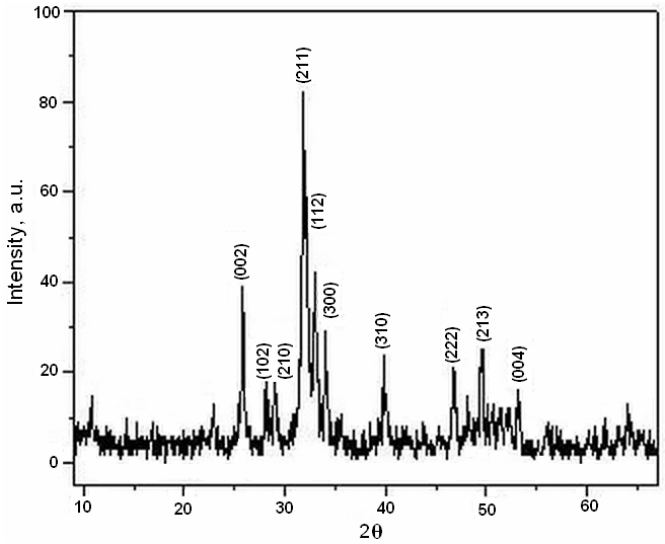

Fig. 1. X-ray diffraction pattern of hydrothermally synthesized CHA powder

The IR spectrum of the synthesized powder (Fig.2.) shows bands characteristic of CHA. The asymmetric stretching (ν3) and bending (ν4) modes of PO_4^{3-} ion were detected at about 1092 and 1042 cm^{-1}, and 603 and 569 cm^{-1}, respectively; while symmetrical stretching modes (ν1 and ν2) of PO_4^{3-} ion were registered at around 957 and 473 cm^{-1}, respectively. The liberation and the stretching mode of OH^- were detected at around 630 and 1626 cm^{-1}, respectively. The stretching vibrations ascribed to CO_3^{2-} at about 1442, 1406 and 875 cm^{-1} are also present. This indicates incorporation of the carbonate group into the apatite structure. The band registered at 630 cm^{-1} is ascribed to the liberation mode of the OH^- vibration. It is evident that type B carbonated hydroxyapatite was obtained and that the replacements at the positions of the OH^- ions, revealed by changes in shape and position of the band at 3658 cm^{-1}, indicate that these changes were not predominantly caused by the substitution of OH^- by CO_3^{2-}.

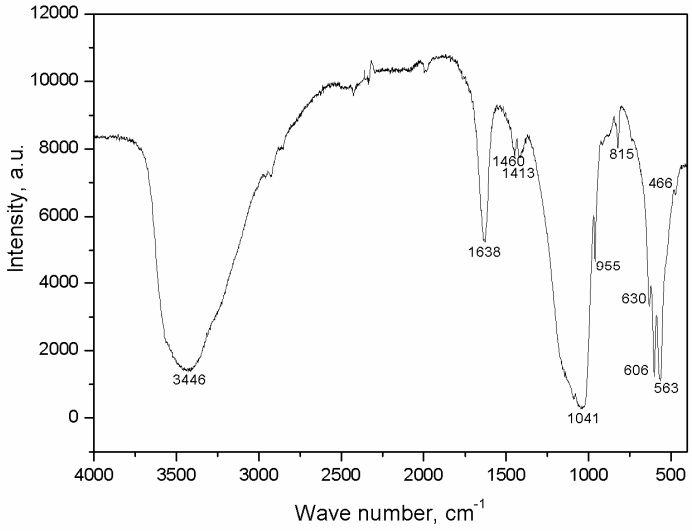

Fig. 2. IR spectrum of hydrothermally synthesized CHA powder

3.2. SEM

CHA powder consists of agglomerates, which are very similar in shape and size (1 - 5μm), as it can be seen on the SEM micrograph (Fig.3.). These agglomerates are built up from fine particles (~200 nm) and their forms are irregular with oval edges due to spherical shapes of individual particles [22].

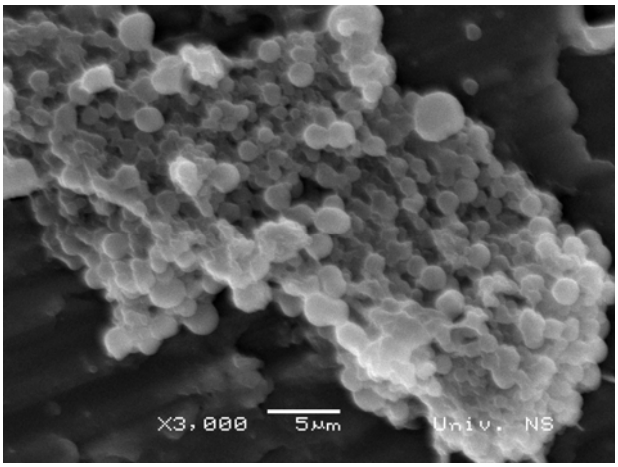

Fig. 3. SEM micrograph of CHA powder

3.3. SBET and porosimetry

Porosity parameters, obtained using BET method, are given in Table I. The average particle diameter, calculated from the specific surface area of CHA powder is 160 nm.

Tab. I Porosity parameters determined by BET method

Sample	S_{BET}, m^2/g	Total pore volume, cm^3/g	Mean pore diameter size, nm
CHA powder	12	1.00	310
Tablet 1, p=16 MPa	13	0.39	75
Tablet 2, p=156 MPa	11	0.17	35

Analyzing differential pore volume plot (Fig. 4), derivatives dV/d(log r) as a function of r, it is possible to completely define the pore distribution in the system. This function connects the pore diameter and partition of corresponding pores, for each discrete value of pore diameter.

Differential pore volume in tablet 1 is significantly higher than that in tablet 2, thus faster drug release is expected from tablet 1 (Fig. 4.).

Pore size distribution and their partition to the total pore volume are given in a histogram (Fig.5.) for easier comparisons.

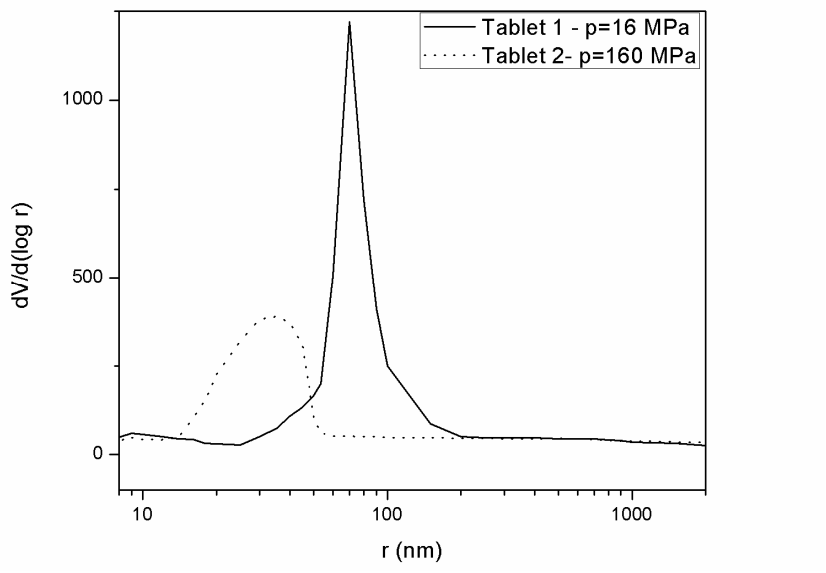

Fig. 4. Differential pore volume

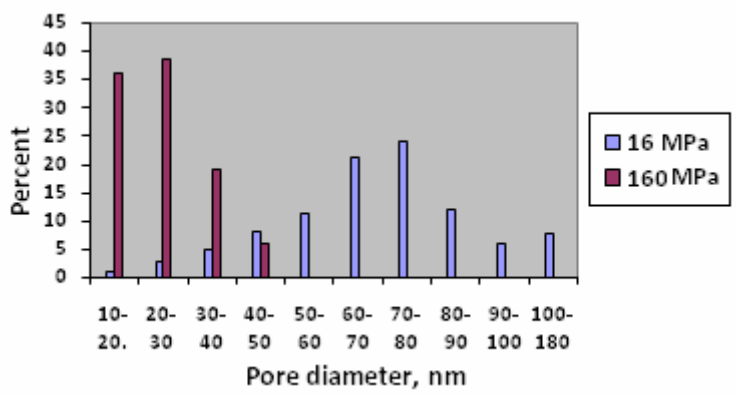

Fig. 5. Pore size distribution and their partition for tablet 1 and 2

Multimodal distribution of pore sizes can be observed in Fig.5. It derives from different types of pores: the largest pores formed during tablet compression, large pores between aggregates, pores between particles, small pores between smaller particles arranged inside of the agglomerates and the smallest pores between basic particles. Comparing pore sizes in tablet 1 (p=16 MPa) and tablet 2 (p=156 MPa), it is evident that the pores in tablet 2 are significantly smaller. In tablet 2, the smallest pores (10-20 nm) contribute in total pore volume with 36 %, while in tablet 1 with only 1.2 %. The most dominant pores in tablet 2 are those with diameters of 20-30 nm, while in tablet 1 those with diameters of 60-80 nm.

3.4. Drug release from tablets

Release profiles of tigecycline from tablets, compressed with different pressures, are shown in Fig.6. The drug release occurs in two stages: first stage is characterized by a fast initial release, and the second by a continuous slow release. This initially high release rate might be of great importance, because the drug effectiveness is often much higher when its concentration at the infection site at the beginning of a therapy is high.

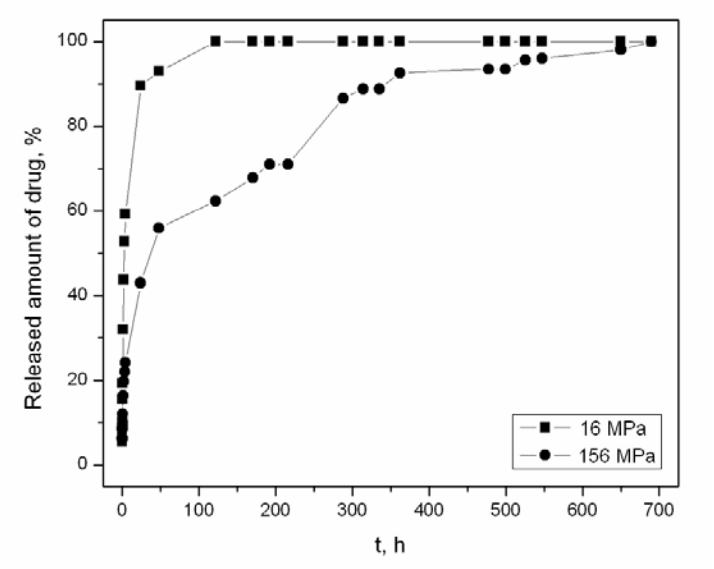

Fig. 6. Release profile of tigecycline

As expected, Higuchi's equation can be applied to the experimental data only when about 60 % of drug has been released. In the case of tablet 1, this equation fits to the experimental data for the period of the first 5 hours when 67% of the total drug amount was released, and in the case of tablet 2, for the period of the first 50 h when 60 % of the drug was released.

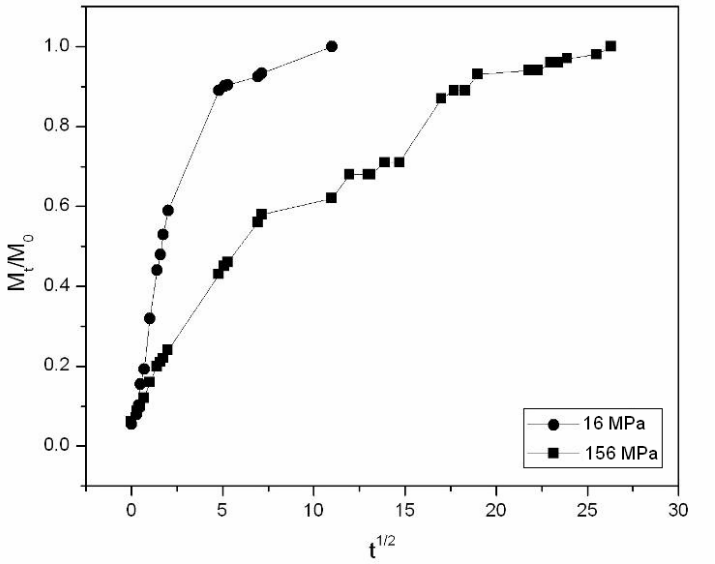

Fig. 7. Fitting data by Higuchi's equation

Appling the Korsmeyer-Peppas equation, in logarithmic form, to tablet 1 data, the same was confirmed, i.e., it fits the data for the initial period of release only, when 67% of the total drug quantity was released (Fig.8.). The coefficient of direction of the linear part of the curve is 0.5, which is also the value of the exponent n. The value of n=0.5 indicates that the Korsmeyer-Peppas equation is reduced to the Higuchi equation (relative release rate proportional to the square root of time). But, as shown, it fits the data for tablet 2 over the whole period of drug release (Fig.8.).

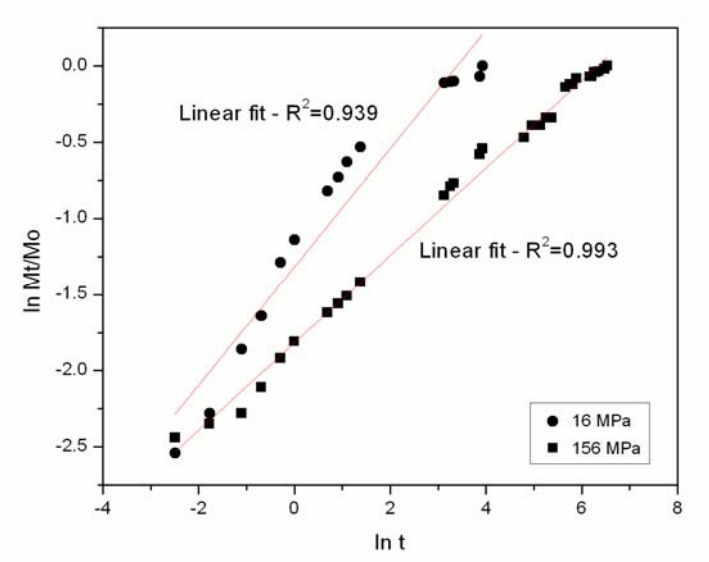

Fig. 8. Fitting data by Korsmeyer-Peppas model

As hydroxyapatite used for fabrication of tablets has a very complex structure (agglomerates (1-5 μm), particles (200 nm), subparticles (160 nm), crystallites (8-22 nm)), the drug release rate can be correlated with the corresponding geometry of apatite particles. Therefore, the relationship between the hierarchical porosity of tablets and the drug release rate was taken as the most essential factor, which has to be carefully analyzed to obtain precise and practical information that would facilitate the designing of various delivery systems for controlled drug release by selecting their optimal geometry.

The tablet porosity data, presented in Fig.5, can be easily correlated with the corresponding drug release rates interpreted by Korsmeyer-Peppas model and given in Fig.8.

In the case of tablet 2 (Fig.8.) we have narrow pore size distribution (10-50 nm) so drug release rate is quite uniform and Korsmeyer-Peppas equation fits the experimental data over the whole period of drug release (R^2=0.993). The coefficient of direction gives the value of release exponent of 0.3.

Opposed to narrow pore size distribution in tablet 2, pore size distribution in tablet 1 is much wider (10-180 nm). Therefore, the kinetics of drug release in this sample can not be described with only one equation. If we observe separately release from the various pores, conditionally named large (60-180 nm), medium (30-60 nm) and small (10-30 nm), then the release kinetics can be described more preciously. Accordingly, the drug release curve for tablet 1 (Fig.8.) can be divided into three linear segments. Each of these segments has different coefficient of direction, which can be assigned to the corresponding drug release rate. Thus, the release is the fastest at the initial stage (coefficient n = 0.5) and is related to the largest pores (with diameter of 60-180 nm and contribution to the total pore volume of 71%). During this period (5 hours), the amount of drug released was approximately 67%. During the next 20 hours, the drug release rate is lower (n = 0.18). The quantity of drug released (about 23%) can be associated with the pores 40-60 nm in diameter (20% of the total pore volume). And finally, the last linear segment, which covers the period of 97 h, shows the lowest release rate (n = 0.008). During this time 10% of the total drug quantity was released. This quantity can be associated with the release from the smallest pores with diameters of 10-40 nm (9% of the total pore volume).

The presented data show that, within any linear interval, the percentage of drug released and the percentage of pores of certain sizes present in the sample is approximately the same. Thus, it follows that the geometry (porosity) is of great importance for the drug release kinetics, and has to be therefore further examined.

4. Conclusions

A new approach to the interpretation of the mechanism of drug release from ceramic materials, which determines the relationship between pore sizes and the drug release rate, was given in this study. Korsmeyer-Peppas model was applied in a modified procedure in order to determine relations between pore sizes, their distribution and drug release rate. This enabled quantification of drug release kinetics based on porosity parameters of the used ceramic device.

It has been shown here that it is possible to predict the rate of drug release from any ceramic device if its porosity is precisely determined.

Acknowledgement

This study was financially supported by the Ministry of Science and Technological Development of the Republic of Serbia (Project No. 172026).

5. References

1. M.P. Ginebra, T. Traykova, J.A. Planell, Calcium phosphate cements as bone drug delivery systems: A review, J. Control. Release 113 (2006) 102–110.
2. W.J.E.M. Habraken, J.G.C. Wolke, J.A. Jansen, Ceramic composites as matrices and scaffolds for drug delivery in tissue engineering, Advanced Drug Delivery Reviews 59 (2007) 234–248.
3. C. Lin, C. Xiao, Z. Shen, Nano Pores Evolution in Hydroxyapatite Microsphere during Spark Plasma Sintering, Science of Sintering 43 (2011) 39-46.
4. Y. Boonsongrit, H. Abe, K. Sato, M. Naito, M. Yoshimura, H. Ichikawa, Y. Fukumori, Controlled release of bovine serum albumin from hydroxyapatite microspheres for protein delivery system, Materials science & engineering B 148 (2008) 162–165.
5. A. K. Jain, R. Panchagnula, Skeletal drug delivery systems, International Journal of Pharmaceutics 206 (2000) 1–12.
6. S. Esposito, S. Leone, Prosthetic joint infections: microbiology, diagnosis, management and prevention, International Journal of Antimicrobial Agents 32 (2008) 287–293
7. N. Fletcher, D. Sofianos, M.B. Berkes, W.T. Obremskey, Prevention of perioperative infection. J. Bone Joint Surg. Am. 89 (2007) 1605–18.
8. A. Slosarczyk, J. Szymura-Oleksiak, B. Mycek, The kinetics of pentoxifylline release from drug-loaded hydroxyapatite implants, Biomaterials 21 (2000) 1215-1221.
9. S. Lepretre, F. Chai, J.C. Hornez, G. Vermet, C. Neut, M. Descamps, H. F. Hildebrand, B. Martel, Prolonged local antibiotics delivery from hydroxyapatite functionalized with cyclodextrin polymers, Biomaterials 30 (2009) 6086–6093.
10. M. Teller, U. Gopp, H.G. Neumann, K.D. Kühn, Release of Gentamicin From Bone Regenerative Materials: An In Vitro Study, Journal of Biomedical Materials Research Part B: Applied Biomaterials 81(2007) 23-29.
11. N.M. Ruiz, E. Gayoso, Y. Vasquez, Tigecycline usage in osteomyelitis caused by multidrugresistent acinetobacter: A report of 10 cases from a single institution, 14th International Congress on Infectious Diseases (ICID) Abstracts, doi:10.1016/j.ijid.2010.02.1932
12. R. Haidar, A. Der Boghossian, B. Atiyeh, Duration of post-surgical antibiotics in chronic osteomyelitis: empiric or evidence-based? International Journal of Infectious

Diseases 14 (2010) 752-758.
13. L.Y. Yin, L. Lazzarini, F. Li, C. M. Stevens, J. H. Calhoun, Comparative evaluation of tigecycline and vancomycin, with and without rifampicin, in the treatment of methicillin resistant Staphylococcus aureus experimental osteomyelitis in a rabbit model, Journal of Antimicrobial Chemotherapy (2005) 55, 995–1002.
14. J. Hylands, Tigecycline: A new antibiotic, Intensive and Critical Care Nursing 24 (2008) 260-263.
15. M.P. Ginebra, T. Traykova, J.A. Planell, Calcium phosphate cements: Competitive drug carriers for the musculoskeletal system, Biomaterials 27 (2006) 2171-2177.
16. R.W. Korsmeyer, R. Gurney, E. Doelker, P. Buri, N.A. Peppas, Mechanisms of solute release from porous hydrophilic polymers, International Journal of Pharmaceutics 15 (1983) 25–35.
17. A.K. Jena, M.C. Chaturvedi, Phase Transformations in Materials, Prentice Hall (1992) p. 247.
18. H. van de Belt, D. Neut, D.R.A. Uges, W. Schenk, J.R. van Horn, H. C. van der Mei, H.J. Busscher, Surface roughness, porosity and wettability of gentamicin-loaded bone cements and their antibiotic release, Biomaterials 21 (2000) 1981-1987.
19. M. Espanol, R.A. Perez, E.B. Montufar, C. Marichal, A. Sacco, M.P. Ginebra, Intrinsic porosity of calcium phosphate cements and its significance for drug delivery and tissue engineering applications, Acta Biomaterialia 5 (2009) 2752–2762.
20. A. Cosijns, C. Vervaet, J. Luyten, S. Mullens, F. Siepmann, L. Van Hoorebeke, B. Masschaele, V. Cnudde, J.P. Remon, Porous hydroxyapatite tablets as carriers for low-dosed drugs, European Journal of Pharmaceutics and Biopharmaceutics 67 (2007) 498–506.
21. M. Oner, E. Yetiz, E. Ay, U. Uysal, Ibuprofen release from porous hydroxyapatite tablets, Ceramics International 37 (2011) 2117–2125.
22. V. Jokanović, D. Izvonar, M. D. Dramićanin, B. Jokanović, V. Živojinović, D. Marković, B. Dačić, Hydrothermal synthesis and nanostructure of carbonated calcium hydroxyapatite, J. Mater. Sci.: Mater. Med. 17 (2006) 539–546.

Садржај: *Кинетика отпуштања тигециклина, потенцијалног антибиотика за лечење остеомијелитиса, из калцијум хидроксиапатита, као једног од најважнијих материјала у инжењерству коштаног ткива, испитивана је у овом раду. Тигециклин, у прашкастом облику, помешан је са прахом ХАП-а и од добијене смеше направљене су таблете, пресовањем под два различита притиска. Ове таблете су урођене у фосфатни пуфер и отпуштање тигециклина је мерено УВ-ВИС спектрофотометра. Укупно време отпуштања било је 5 или 28 дана, у зависности од примењеног притиска пресовања. Показало се да постоји блиска веза између величине пора и брзине отпуштања лека. Кинетика отпуштања лека је интерпретирана са аспекта величине пора и расподеле величине пора.*

Кључне речи: *хидроксиапатит, геометрија пора, отпуштање лека*